



# Compressive strength evaluation of cement-based materials in sulphate environment using optimized deep learning technology

Yang Yu<sup>a,b</sup>, Chunwei Zhang<sup>a,\*</sup>, Xingyang Xie<sup>c,d</sup>, Amir M. Yousefi<sup>e</sup>, Guang Zhang<sup>f</sup>, Jiehong Li<sup>b</sup>, Bijan Samali<sup>e</sup>

<sup>a</sup> Multidisciplinary Center for Infrastructure Engineering, Shenyang University of Technology, Shenyang, Liaoning, 110870, China

<sup>b</sup> Centre for Infrastructure Engineering and Safety, School of Civil and Environmental Engineering, University of New South Wales, Sydney, NSW, 2052, Australia

<sup>c</sup> Taizhou Customs Comprehensive Technical Service Center, Taizhou, Zhejiang, 318000, China

<sup>d</sup> Faculty of Mechanical Engineering & Mechanics, Ningbo University, Ningbo, Zhejiang, 315211, China

<sup>e</sup> School of Engineering, Design and Built Environment, Western Sydney University, Penrith, NSW, 2747, Australia

<sup>f</sup> College of Mechanical Engineering, Zhejiang University of Technology, Hangzhou, Zhejiang, 310014, China

## ARTICLE INFO

### Keywords:

Cement-based materials  
Compressive strength  
Deep learning  
Convolutional neural network  
Particle swarm optimization

## ABSTRACT

Strength serves as a vital performance metric for assessing long-term durability of cement-based materials. Nevertheless, there is a scarcity of models available for predicting residual strength of in-situ structures made of cement-based materials exposed to sulphate conditions. To address this challenge, this study presents a novel approach using deep learning to predict the degradation of compressive strength of cement-based materials under marine environments. Specifically, a deep convolutional neural network (DCNN) is established, consisting of two convolutional layers, one pooling layer, and two fully connected layers. In this innovative model, contents of cement, water-to-cement ratio, sand, sulphate concentration and exposure temperature are selected as inputs, while the output is strength of cement-based materials subjected to sulphate deterioration. To improve the forecast capability, particle swarm optimization is adopted for optimizing hyperparameters of DCNN, which can be implemented by reducing the discrepancy between model prediction and measured strength. Finally, experimental data are used to establish and evaluate proposed method. The results show that the proposed deep learning-based predictive model has the best performance of strength degradation prediction of cement-based materials suffering from sulphate attack via a comparison with other commonly used models. The outcome of this research offers a potential solution for predicting remaining strength of cement-based materials that undergo practical sulphate attack.

## 1. Introduction

Concrete is a widely used and versatile material in civil engineering and industrial facilities. Its importance lies in its structural capacity, durability, and ability to withstand different loads and environmental conditions (Surehali et al., 2023; Ting and Ting, 2023). The strength of concrete is a critical property that determines its quality and suitability for a particular application. Concrete strength is determined by several factors, including the composition of the materials used, the curing process, and environmental exposure (Akbar and Liew, 2021; Yin et al., 2023). In challenging environments, such as those rich in sulphates, concrete can experience a rapid deterioration in performance, which can compromise the safety and durability of civil structure (Chen et al.,

2018a; Yao and Chu, 2023). The presence of sulphate ions in the soil or groundwater can react with the calcium hydroxide in the concrete, leading to the formation of expansive compounds that can cause cracks and weaken the concrete structure (Yu et al., 2023). Therefore, it is essential to assess the suitability of concrete mix designs for specific environments to ensure long-term performance and safety. Compressive strength is frequently the key metric used to assess the quality and safety of pre-existing concrete structures (Akbar et al., 2021). It is the maximum load that concrete can bear before it fails in compression. Regularly monitoring the strength of concrete during its serviceable life is able to provide valuable information for quality control, performance maintenance, and early detection of potential problems (Ji et al., 2023). Additionally, predicting concrete strength can help assess the structural

\* Corresponding author.

E-mail address: [zhangchunwei@sut.edu.cn](mailto:zhangchunwei@sut.edu.cn) (C. Zhang).

<https://doi.org/10.1016/j.dibe.2023.100298>

Received 28 June 2023; Received in revised form 10 November 2023; Accepted 3 December 2023

Available online 8 December 2023

2666-1659/© 2023 The Authors. Published by Elsevier Ltd. This is an open access article under the CC BY-NC-ND license (<http://creativecommons.org/licenses/by-nc-nd/4.0/>).

degradation of concrete over time and improve its safety (Moutassem, 2022). Despite the critical role that concrete strength plays in ensuring the safety and longevity of structures, the ability to forecast and evaluate the actual strength of concrete in real-time remains a challenging task. This is owing to the intricate degradation mechanisms and numerous contributing factors that affect concrete strength in different environments (Bone et al., 2022). Although several endeavors have been made to formulate predictive models for concrete strength, there is currently no universally accepted method to estimate compressive strength of materials on basis of cement in severe or challenging environments. Further research is necessary to develop effective methods for predicting concrete strength and improving the durability and safety of concrete structures in challenging environments.

There are currently two types of methods to estimate the level of compressive strength in concrete. The initial approach is the conventional mathematical and statistical forecasting method, which necessitates an extensive dataset (Mohammed et al., 2020a; Sarwar et al., 2019b). While it may provide accurate projections with an infinite dataset, the number of available samples is frequently restricted in reality. The second type pertains to nonlinear forecasting techniques, which do not have a unified mathematical theory and tend to generate optimal solutions that are partial in nature, rather than global in scope (Mohammed and Mahmood, 2021; Sarwar et al., 2019a). While both types are capable of being employed to predict traditional concrete compressive strength, for concrete that is subjected to sulphate assault, the relationship between the input factors and compressive strength becomes highly complex and nonlinear with an increase in the number of input variables. Therefore, predicting compressive strength values of concrete in severe or challenging environments using regression models is not suitable. As a result, models based on artificial intelligence (AI) have received more attention (Koopialipour et al., 2022). Artificial neural networks (ANN) and other machine learning (ML) techniques have gained prominence as a research field for simulating the strength of concrete materials (Congro et al., 2021; Liang et al., 2018; Nazar et al., 2023; Tahwia et al., 2021). Mohammed et al. (2021a) developed ANN model and M5P model to predict the compressive strength of concrete incorporate with two kinds of polymer. Similarly, ANN and other ML models have been established to model the strength of cement-based mortar with different curing time and ratios of water to cement ratio (Mohammed et al., 2020b). Mohammed et al. (2023) utilised ANN to investigate impact of curing temperature on compressive strength of concrete including ground granulated blast furnace slag. Modeling strength performance of green concrete with high volume fly ash was also investigated by using ANN (Mohammed et al., 2021b). Jaf et al. (2023) employed ANN to analyze the influence of CaO and SiO<sub>2</sub> on compressive strength of fly ash-based concrete. Ahemd et al. (2022) proposed a novel surrogate model based on ANN to evaluate the strength of alkali activated binder concrete involving nano silica.

An ANN model comprises inputs, weights, a summing function, an activation function, and outputs. The optimal number of neurons and layers in the hidden layer, as well as various learning parameters, are required by different algorithms. The backpropagation (BP) algorithm is commonly used to train ANN models by adjusting connection weights and bias values during the training process (Zhang et al., 2023). However, ANN models have some limitations. Firstly, they cannot offer details on the degree of significance of each parameter. Secondly, it is challenging to determine a logical explanation for the entire network framework. Additionally, ANN models have intrinsic limitations, such as gradual convergence rate, poor generalization effects, reaching local minimums, and overfitting problems (Lyu et al., 2022). These limitations imply that ANN models may not always provide satisfactory results, and they require careful consideration and analysis before being used in real-world applications.

As a subset of ML, deep learning technologies have been quickly developed in past few years, with the ability to acquire knowledge from extensive quantities of data and make accurate predictions (Yu et al.,

2023b). Using complex algorithms for analysing and interpreting data, deep learning has a wide range of applications across different domains, such as natural language processing (Dharaniya et al., 2023), computer vision (Yu et al., 2023a), speech recognition (García-Salinas et al., 2023), and autonomous systems (Gao et al., 2022), among others. Recently, deep learning has found several applications in the field of construction materials, particularly in the areas of material characterization (Lux et al., 2023), quality control (Zeng et al., 2022), automated microscopy analysis (Hilloulin et al., 2022), crack detection (Hao et al., 2023) and property prediction (Deng et al., 2018). Lux et al. (2023) designed a new network architecture to accurately estimate the mass, class and binary mask of recycled aggregates using 2D images. The proposed technology has the potential to replace manual sorting tests and other geometric characterization tests, such as particle size distribution analysis, which makes it possible to monitor the composition of recycled aggregates in real-time. Zeng et al. (2022) employed deep learning to segment and examine spherical particles of fly ash, using a basic optical microscope and a path aggregation network. The proposed approach is able to effectively detect microspheres and predict their particle size distribution and volume fraction, surpassing the capabilities of conventional methods for particle analysis, the results of which are directly correlated with important properties that affect the overall quality of fly ash. Hao et al. (2023) introduced a precise and fully automated approach for semantically segmenting multi-cracks in engineered cementitious composites (ECCs), utilizing a deep learning method with dual pre-modification that takes into account the unique characteristics of the task at hand. The suggested approach is easier to comprehend compared to conventional digital image correlation technique, which results in a significant increase in the accuracy of crack classification, from 92.28% to 99.87%. Although deep learning has been proven to be effective in dealing with complex engineering problems, it is still challenging to tune hyperparameters of deep learning models, which play a critical role in determining the accuracy, speed, and generalization ability of a neural network. Selecting optimal hyperparameters is crucial for achieving high performance, preventing overfitting or underfitting, and reducing training time.

The aim of this study is to investigate the capability of deep learning in modeling compressive strength of cement-based materials undergone sulphate deterioration. In contrast to conventional ML models characterized by shallow structures, deep learning-based models amalgamate the dual tasks of feature extraction and pattern recognition within a single and more intricate learning module. This profound architecture empowers deep learning models to effectively manage unstructured data by acquiring high-level abstract representations. Consequently, when juxtaposed with traditional machine learning models, they prove exceptionally well-suited for elucidating the intricate and highly complex relationships between the influencing factors and compressive strength of cement-based materials subjected to sulphate attack. This affords a deeper and more comprehensive understanding of these complex interconnections. To start with, a comprehensive dataset, comprising cement content, ratio of water to cement, fine aggregate, sulphate concentration, superplasticizer, exposure time and compressive strength of cement mortar, was collected from the literature. Then, a CNN with deep architecture (DCNN) is built up as the predictive model to assess compressive strength of cement-based materials that have undergone sulphate deterioration, where collected data is employed for both training and testing purposes to establish the model accuracy. It is well known that the performance of DCNN model in predicting mechanical strength of cement-base materials subjected to sulphate attack is heavily dependent on the setting of network hyperparameters. Inaccurate hyperparameters settings can give rise to undesirable outcomes such as over-fitting and over-fitting in DCNN models. It is of great importance to note that varying combinations of hyperparameters can yield markedly different performance in trained models. Consequently, the pursuit of optimal hyperparameter values is a crucial and fundamental aspect when developing a DL model. By diligently seeking and

fine-tuning these values, it can be guaranteed that the developed DCNN model performs at its best and effectively addresses the problem of strength prediction of cement-based materials under severe environmental conditions. In this research, to achieve this target, improved particle swarm optimization (IPSO) algorithm is employed to optimize network hyperparameters. The capability of suggested method is confirmed by means of several statistical metrics, including R-squared ( $R^2$ ), mean absolute percentage error (MAPE), root mean square error (RMSE), and mean absolute error (MAE), via the comparison with that of other prestigious ML approaches. Finally, the robustness and sensitivity analyses are conducted to demonstrate the effectiveness of this innovative method in compressive strength prediction of cement-based materials subjected to sulphate attack.

## 2. Conceptual framework

### 2.1. Convolutional neural networks

Convolutional Neural Network (CNN) is a type of deep neural network that is commonly used for processing and analyzing structured grid-like data, such as images, videos, and time series data (Gu et al., 2018; Yu et al., 2022). It has revolutionized the field of computer vision and has been widely used in various applications, including image recognition, object detection, data reconstruction, etc. The key feature of CNNs is their ability to automatically learn and extract hierarchical patterns and features from input data (Zhang et al., 2022). This is achieved through the use of convolutional layers, pooling layers, and fully connected (FC) layers.

Convolutional layers perform the core operation of convolution. They consist of a set of learnable filters (also known as kernels) that slide over the input data, computing dot products between the filter weights and the input values. The result is a feature map that highlights important patterns and local dependencies in the data. Pooling layers are used to reduce the spatial dimensions of the feature maps produced by convolutional layers. The most common pooling operation is max pooling, which selects the maximum value from a local neighborhood. Pooling helps in creating a spatial hierarchy and achieving translation invariance. FC layers are typically placed at the end of the network and are responsible for making predictions based on the high-level features extracted by the convolutional layers. Each neuron in an FC layer is connected to all the neurons in the previous layer, allowing for complex relationships to be learned.

The general formula for a convolutional layer is as follows:

$$C_i = \sigma \left( \sum_{j=1}^F \omega_j * C_{i-1,j} + b_i \right) \quad (1)$$

where  $C_i$  is the  $i$ th feature map;  $F$  is the number of filters in the convolutional layer;  $\omega_j$  is the  $j$ th filter;  $C_{i-1,j}$  is the  $j$ th feature map from the previous layer; “\*” denotes the convolution operation;  $b_i$  is  $i$ th bias term;  $\sigma$  is the activation function.

The general formula for a max pooling layer is as follows:

$$P_{i,j} = \max_{(m,n) \in R_{i,j}} C_{i,m,n} \quad (2)$$

where  $P_{i,j}$  is the output of the  $i$ th max pooling layer and  $j$ th feature map;  $R_{i,j}$  is the receptive field of the  $i$ th max pooling layer and  $j$ th feature map;  $C_{i,m,n}$  is the input to the  $i$ th max pooling layer and  $j$ th feature map at position  $(m,n)$ .

The general formula for FC layer is as follows:

$$y = \sigma(Wx + b) \quad (3)$$

where  $y$  is the output of the FC layer;  $W$  is the weight matrix;  $x$  is the input vector of FC layer;  $b$  is the bias vector.

### 2.2. Improved particle swarm optimization

Particle swarm optimization (PSO) is a metaheuristic optimization algorithm inspired by the social behavior of bird flocking and fish schooling. It was first introduced by Kennedy and Eberhart (1995). The basic idea of PSO is to mimic the social behavior of a group of particles (or agents) in a search space by adjusting their positions and velocities based on their own experience and the experience of the entire swarm (Zhang, 2023).

The PSO algorithm maintains a population of particles, where each particle represents a candidate solution in the search space. The position of a particle in the search space is represented by a vector  $x_i = (x_{i1}, x_{i2}, \dots, x_{in})$ , where  $n$  is the dimensionality of the search space. The velocity of a particle is represented by another vector  $v_i = (v_{i1}, v_{i2}, \dots, v_{in})$ , which determines the direction and speed of the particle movement in the search space. The movement of each particle in the swarm is determined by two rules: personal best ( $pbest$ ) and global best ( $gbest$ ). The personal best rule updates the particle position based on its own best position so far, while the global best rule updates the particle position based on the best position found by any particle in the swarm. The position and velocity of a particle at time  $t+1$  are updated using the following equations:

$$v_i(t+1) = w \bullet v_i(t) + c_1 \bullet rand \bullet (pbest_i - x_i(t)) + c_2 \bullet rand \bullet (gbest - x_i(t)) \quad (4)$$

$$x_i(t+1) = x_i(t) + v_i(t+1) \quad (5)$$

where  $w$  is the inertia weight,  $c_1$  and  $c_2$  are acceleration coefficients,  $rand$  is a random number between 0 and 1,  $pbest_i$  is the personal best position of particle  $i$ , and  $gbest$  is the global best position found by any particle in the swarm. The inertia weight  $w$  determines the balance between the particle current velocity and its previous velocity. The acceleration coefficients  $c_1$  and  $c_2$  determine the influence of the particle's personal best and global best on its movement. The PSO algorithm terminates when a stopping criterion is met, such as a maximum number of iterations or a satisfactory solution is found.

Even though there have been some enhancements made to the PSO algorithm, the issue of premature convergence remains a major drawback in all of the improved versions (Nguyen et al., 2019). To prevent the particles from getting trapped in a local optimal value too early, this section introduces an improved PSO (IPSO) algorithm. Compared to the standard PSO, this new algorithm incorporates two key improvements that address the issue of premature convergence.

The first improvement is about inertia weight  $w$ , which affects the updating trend of particle velocity and position. The larger the inertia weight, the stronger the global optimization ability and the weaker the local optimization ability; the smaller the value, the weaker the global optimization ability and the stronger the local optimization ability. In the process of using PSO to search for the optimal solution, the smaller the fitness value, the closer it is to the optimal solution, and the stronger the local search ability, that is, the need to reduce  $w$ ; the larger the fitness value, the farther it is from the optimal solution, and the greater the need for global search, that is, the need to increase  $w$ . Accordingly, the change of  $w$  has a direct impact on fitness value of a particle. In PSO, it is important to adjust the inertia weight  $w$  in accordance with the fitness value during the iterative optimization process. This helps to maintain a balance between the particle search speed and the overall optimization ability. As such, fixing the value of the inertia weight  $w$  as a constant is not an effective way to optimize the algorithm. Instead, real-time adaptation of the inertia weight  $w$  is more beneficial in addressing reactive power optimization problems. Consequently, an adaptive inertia weight is proposed, with the following expression:

$$w(it) = w_{min} + (w_{max} - w_{min}) e^{-a_1 \left( \frac{it}{Miter} \right)^{a_2}} \quad (6)$$

where  $w_{min}$  and  $w_{max}$  are minimal and maximal inertia weights,

respectively;  $it$  and  $Miter$  are current and maximal iteration numbers, respectively;  $a_1$  and  $a_2$  are two factors regarding slope and symmetry of curve, respectively.

The second modification of PSO is for acceleration coefficients, i.e., individual acceleration coefficient  $c_1$  and swarm acceleration coefficient  $c_2$ .  $C_1$  represents the best result that an individual has found during its search, while  $c_2$  is a value used to compare the best results discovered by all individuals. Therefore, in the early stage of the algorithm, it is necessary to increase  $c_1$  to ensure solution diversity. In the later stage of the algorithm, it is necessary to increase  $c_2$  to quickly find the optimal solution. Hence, to meet the different requirements for  $c_1$  and  $c_2$  in different optimization stages, dynamic adjustment parameters will be introduced to change  $c_1$  and  $c_2$  in real-time, in order to achieve a higher level of optimization accuracy. The relevant formulas are given as follows:

$$c_1(it) = c_1^{min} + \frac{it \cdot (c_1^{max} - c_1^{min})}{Miter} \tag{7}$$

$$c_2(it) = c_2^{min} + \frac{it \cdot (c_2^{max} - c_2^{min})}{Miter} \tag{8}$$

where  $c_1^{min}$  and  $c_2^{min}$  are minimum values of  $c_1$  and  $c_2$ , respectively, and  $c_1^{max}$  and  $c_2^{max}$  are maximum values of  $c_1$  and  $c_2$ , respectively.

### 3. Data collection and analysis

The experimental data used in this research for model development and evaluation is from the study conducted by [Chen et al. \(2018b\)](#). In the experiment, three different types of mortar were formulated using water-to-cement ratios of 0.65, 0.50, and 0.28, respectively. To test the freshly prepared mortar, it was poured into a  $40 \times 40 \times 160$  mm steel mold and compacted on a vibrating table. Once the samples were compacted, they were demolded within 24 h of pouring. To ensure proper curing, the specimens were then cured for a period of 90 days in a curing chamber that is carefully regulated to maintain a temperature range of  $20 \pm 2$  °C and a relative humidity level exceeding 95%. This extended curing period allowed the mortar to achieve its maximum strength and durability, which is essential for reliable and long-lasting construction.

After the 90-day curing period, the test specimens underwent degradation testing in a controlled environment with precise temperature and humidity parameters. The chamber maintained a temperature range of 20–80 °C and a humidity range of 50%–95%, ensuring that the conditions remained consistent throughout the experiment. The corrosion solution used in the test was sodium sulphate, with varying concentrations of 2%, 10%, and 16.3%, respectively. The use of different concentrations allowed for a comprehensive evaluation of the concrete resistance to corrosion under varying levels of chemical exposure. To accelerate the degradation process, the wet-dry cycle method was employed. This method involved immersing the concrete specimens in the corrosion solution for 8 h at a temperature of  $20 \pm 2$  °C, followed by drying them for 16 h at  $50 \pm 2$  °C under a relative humidity of 60%. This cycle was repeated multiple times to simulate the long-term effects of natural weathering and chemical exposure on the concrete. A compressive strength test was carried out on the specimen using axial compression. Three specimens were tested for each deterioration age, and the compression was performed at a rate of 2.4 kN/s. The detailed design, fabrication and test of specimens can be found in ([Chen et al., 2018b](#)).

The above experimental program generated a total of 638 groups of data, containing information of cement percentage, water-to-cement ratio (w/c), sand percentage, superplasticizer percentage (SP), sulphate concentration (SSC) and exposure time (ET), and corresponding strength (CS) of mortar specimen. [Table 1](#) displays the statistical analysis results of the entire dataset, which include minimum, maximum,

**Table 1**  
Statistical analysis result of dataset.

Parameter	Minimum	Maximum	Mean	STD
w/c	0.28	0.65	0.47	0.15
Cement (%)	18	30.63	23.43	5.37
Sand (%)	60.81	70	66.24	3.990
SP (%)	0	2	0.67	0.97
SSC (%)	2	16.3	9.28	5.85
ET (day)	0	360	175	104
CS (MPa)	3.17	90.45	50.64	25.02

mean and standard deviation (STD) of each component. It is evident that all the parameters contain large ranges, ensuring that the predictive model developed based on this dataset possesses generality and wide applicability. Then, the dataset is randomly divided into two subsets for model training and testing on basis of ratio of 70%–30%. Before the predictive model is established, the model inputs should be assessed to avoid redundant information. Here, we use the correlation coefficient to quantify the dependency between any two input variables. If the absolute value of correlation coefficient of two variables is above 0.8, we consider that these two variables have a strong dependency, with redundant information. One variable should be removed to reduce the input dimension. [Fig. 1](#) depicts the correlation coefficient of any two variables in the form of matrix. It is clearly seen that all the absolute values of correlation coefficients are below 0.7, except that on the diagonal of matrix, which indicating self-correlation of variables. Accordingly, we will include all six influence factors as input variables to build up the predictive model of strength degradation of cement-based materials in sulphate environment, which will be presented in detail in next section.

### 4. Proposed improved PSO-optimized DCNN for compressive strength prediction of cement-based materials subjected to sulphate attack

This study puts forward a novel data-driven model for predicting compressive strength of cement-based materials subjected to sulphate attack using DCNN architecture, as illustrated in [Fig. 2](#). The model comprises an input layer with 2D matrix, two convolutional layers, a pooling layer, two FC layers, and an output layer. The input layer has a size of  $2 \times 3$ , incorporating six variables, namely C, w/c, S, SP,  $SO_4^{2-}$  and ET. The first convolutional layer, named as Conv1, consists of 16 kernels with a kernel size of  $1 \times 2$ , a stride size of 1, and a padding size of 1. Following this, a max-pooling layer is added to downsample the learned

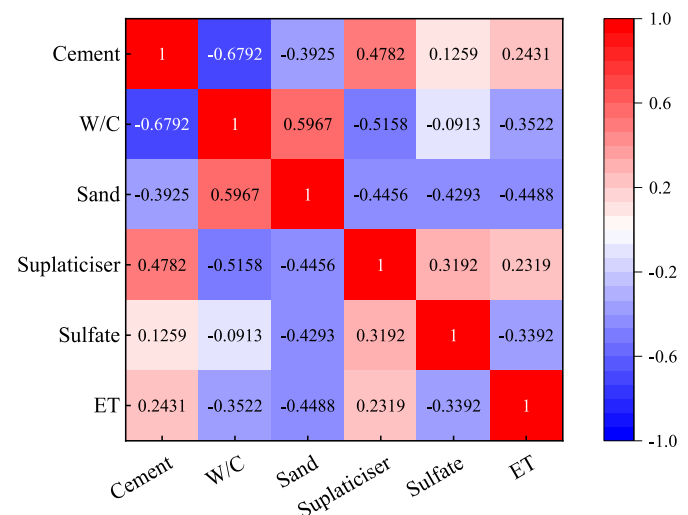


**Fig. 1.** Correlation coefficient matrix of six input variables.

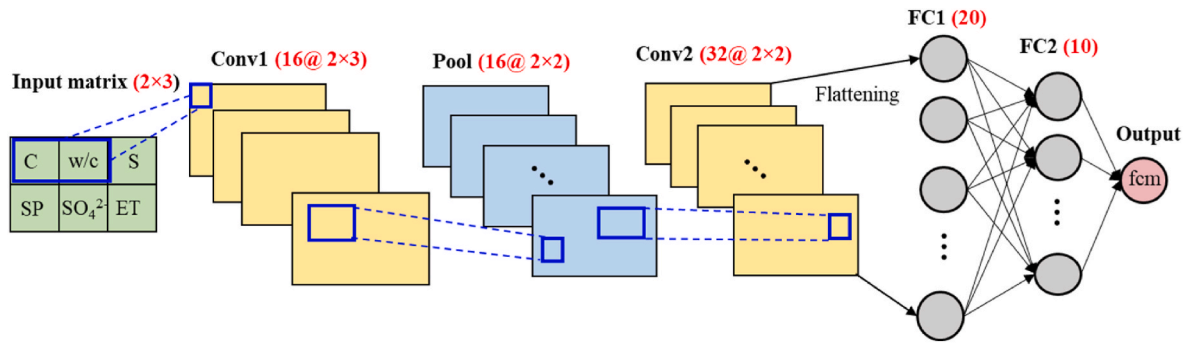


Fig. 2. Architecture of proposed DCNN model for strength prediction of cement-based materials subjected to sulphate attack.

representations, as it has been demonstrated to be more effective than average pooling. The pooling layer has a kernel size of  $1 \times 2$ , a stride size of 1, and a padding size of 0. Subsequently, the second convolutional layer, named as Conv2, with 32 kernels is added to explore deeper features that are sensitive to the compressive strength deterioration of cement mortars in sulphate environment. This layer also has a kernel size of  $1 \times 2$ , a stride size of 1, and a padding size of 1. Two FC layers, namely FC1 and FC2, are then connected to Conv2. FC1 is used to flatten the 2D representation to a one-dimensional feature map, and its output is passed to FC2, which compresses the flattened features and reduces their dimensions. FC1 and FC2 are considered hidden layers for optimal feature selection during the mapping process. The number of neurons in FC1 and FC2 are 20 and 10, respectively, which is a way of reducing redundant and unnecessary features. To prevent overfitting due to multiple hidden neurons in FC layers, dropout is performed between Conv2 and FC1. This technique randomly suppresses some neurons, increasing the diversity of the DCNN.

Because the prediction capability of proposed DCNN model is significantly impacted by the hyperparameters, IPSO is utilised to seek out the best values of hyperparameters during model training, including dropout coefficient  $d_1$ , primary learning rate ( $\gamma$ ),  $\gamma$  drop factor ( $\gamma_1$ ),  $\gamma$  drop period ( $\gamma_2$ ), weight deterioration coefficient ( $wd_1$ ), and momentum  $m_1$ . The type and tuning scale of each hyperparameter is displayed in Table 2. The hyperparameter tuning here can be deemed as an optimization process, where the optimization goal (fitness) is defined as the root mean square error (RMSE) between experimentally measured strength and model predictions, the formula of which is shown in Eq. (9):

$$RMSE = \frac{1}{n_t} \sum_{i=1}^{n_t} [f_{st}(i) - \hat{f}_{st}(i)]^2 \quad (9)$$

where  $n_t$  denotes the number of training data, and  $f_{st}$  and  $\hat{f}_{st}$  denote the measured and predicted strengths of cement-based materials subjected to sulphate attack, respectively.

The procedure of IPSO to optimize the hyperparameters of CNN model for predicting compressive strength of cement-based materials subjected to sulphate attack can be summarized as the following steps, which are also presented in the flowchart in Fig. 3.

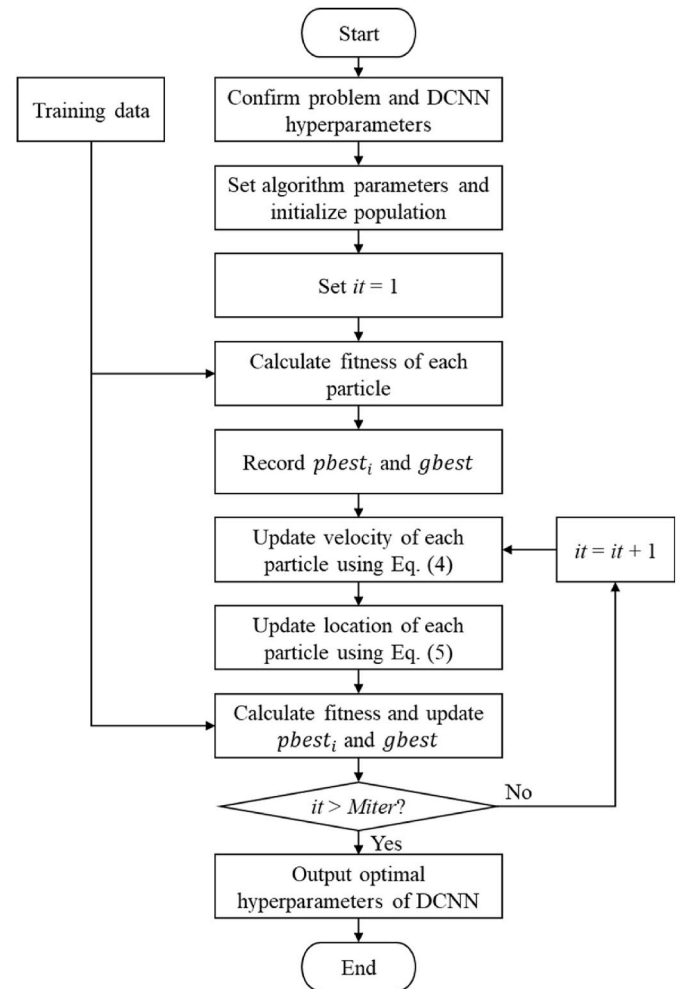


Fig. 3. Flowchart of hyperparameter optimization of DCNN using IPSO.

Step 1 Identify the objective function to be optimized, which is Eq. (9), and determine the search space boundaries and the dimensionality of the problem.

Step 2 Set the algorithm parameters of IPSO.

Step 3 Initialize the swarm. Calculate the fitness value of each particle in the swarm, and record the individual and global best positions.

Step 4 Update the velocity and position of each particle using Eq. (4) to Eq. (8), and then recalculate the fitness values for individual and global best positions.

Step 5 Compare the current individual and global best positions with previous ones. If current positions are better than previous ones,

Table 2  
Hyperparameters of DCNN to be optimized.

Parameter	Type	Minimum	Maximum
$d_1$	Decimal	0.1	0.9
$\gamma$	Decimal	1e-4	0.1
$\gamma_1$	Decimal	0	1
$\gamma_2$	Integer	5	15
$wd_1$	Decimal	0.01	0.9
$m_1$	Decimal	0	1

update corresponding positions; otherwise, keep the best positions unchanged.

Step 6 Check if the termination criteria are met. In this study, the termination condition is whether the algorithm arrives at its maximum iteration number. If so, terminate the algorithm iteration and output optimal network hyperparameters; otherwise, go back to Step 4 for next round of iteration.

The schematic diagram illustrating the overall flowchart of this study is depicted in Fig. 4.

### 5. Results and discussion

In this research, the proposed DCNN model and IPSO algorithm are coded using Matlab v.2022b, where deep learning and optimization toolboxes are employed. For the purpose of model development and evaluation, the whole dataset is divided into two groups for model training and testing, based on the ratio of 70%–30%. To mitigate the impact of varying input variable scales and improve the stability and robustness of the trained model, data normalization is applied to both the training and test datasets, as outlined in Eq. (10):

$$in\_v_i^{norm} = \frac{in\_v_i - \mu_i}{\sigma_i} \tag{10}$$

where  $in\_v_i$  denotes  $i$ th input variable,  $\mu_i$  denote the mean of  $i$ th input variable, and  $\sigma_i$  denotes the standard deviation of  $i$ th input variable.

During the training procedure, IPSO is adopted to optimize the model hyperparameters, including  $d_1$ ,  $\gamma$ ,  $\gamma_1$ ,  $\gamma_2$ ,  $wd_1$  and  $m_1$ . Here, the parameters in IPSO is set as follows: swarm size is 30,  $Miter = 200$ ,  $w_{min} = 0.1$ ,  $w_{max} = 0.9$ ,  $a_1 = 10$ ,  $a_2 = 5$ ,  $c_1^{min} = c_2^{min} = 1$ , and  $c_1^{max} = c_2^{max} = 2$ . To showcase exceptional capability of IPSO to optimize DCNN model for predicting the strength of cement-based materials exposed to sulphate attack, we compare IPSO with PSO and GA, evaluating them based on fitness and convergence. To ensure a fair comparison, the swarm (population) numbers and maximum iteration numbers of PSO and GA are set to match that of IPSO. Additionally, in PSO, the inertia weight factor is set to 0.6, with learning rates  $c_1 = c_2 = 1.5$ . In GA, crossover and mutation coefficients are set to 0.85 and 0.15, respectively, and roulette wheel selection strategy is employed. Fig. 5 demonstrates the comparison of three algorithms in optimizing DCNN hyperparameters for strength prediction. It is evident that PSO exhibits the fastest convergence among three algorithms but results in premature convergence, leading to the highest fitness. On the other hand, while the proposed IPSO converges more slowly, it ultimately performs the best owing to excellent refinement ability in the later stage of algorithm evaluation. Hence, it can be concluded that the IPSO outperforms both PSO and GA in optimizing hyperparameters of DCNN for predicting the strength of cement-based materials subjected to sulphate attack. The DCNN hyperparameters optimized by IPSO are summarized in Table 3.

Based on the best network hyperparameters, the DCNN model for predicting strength of cement-based materials under sulphate environment is established. Then, both training and test data are sent to the

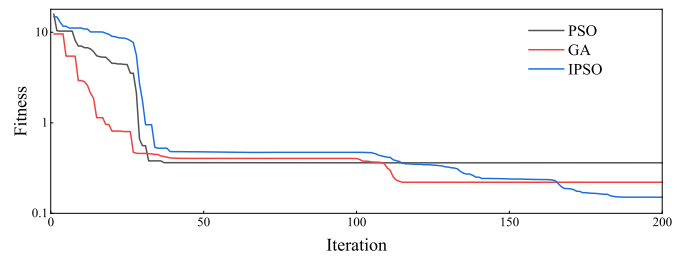


Fig. 5. Comparison of three algorithms for optimizing DCNN hyperparameters.

Table 3

Optimal hyperparameters of DCNN for strength prediction of cement-based materials subjected to sulphate attack.

Parameter	$d_1$	$\gamma$	$\gamma_1$	$\gamma_2$	$wd_1$	$m_1$
Value	0.674	0.012	0.141	7	0.003	0.903

trained model for performance evaluation. Fig. 6 illustrates a comparison between the experimentally measured strength and the predicted strength using the proposed hybrid method. The comparison is based on sequential responses for both the training and test data. It is evident that the proposed model accurately predicts the strength of cement-based materials under sulphate attack, as demonstrated by the nearly identical responses.

To provide further evidence of the superiority of the proposed method compared to existing models, we conducted a comparative study. We compared the proposed method with other commonly used ML models in concrete area, namely ANN, support vector machine (SVM) (Ling et al., 2019), Gaussian process regression (GPR) (Ly et al., 2022), and ensemble decision tree (EDT) (Li and Song, 2022), for predicting the compressive strength of cement-based materials under sulphate attack. In order to ensure a fair comparison, we optimized the hyperparameters of these ML models using IPSO during the training process. The hyperparameters and their corresponding optimization results for each ML model are presented in Table 4.

Next, we utilize the coefficient of determination ( $R^2$ ), a statistical measure that indicates the degree of agreement between experimentally measured strength and predicted strength, to evaluate the performance of the different models. Generally,  $R^2$  ranges from 0 to 1, where a value of 0 represents poor performance, and a value of 1 signifies an excellent capability of the evaluated model. The results of the model performance, analyzed through regression analysis, are illustrated in Figs. 7–11. It is worth noting that both the training and test data points of all the models are evenly scattered around the regression line  $y = x$ , suggesting exceptional prediction accuracy. Among the five models examined, the proposed IPSO-optimized CNN model exhibits the best performance, achieving  $R^2$  values of 0.9999 and 0.9998 for the training and test data, respectively.

To further assess the exceptional predictive capability of the developed model for predicting the strength of cement-based materials under

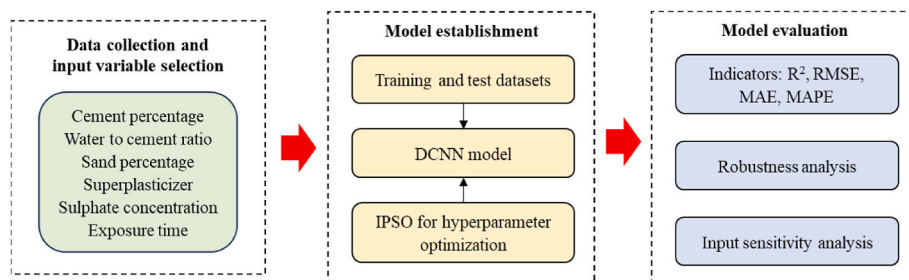


Fig. 4. Schematic diagram for overall flowchart of this study.

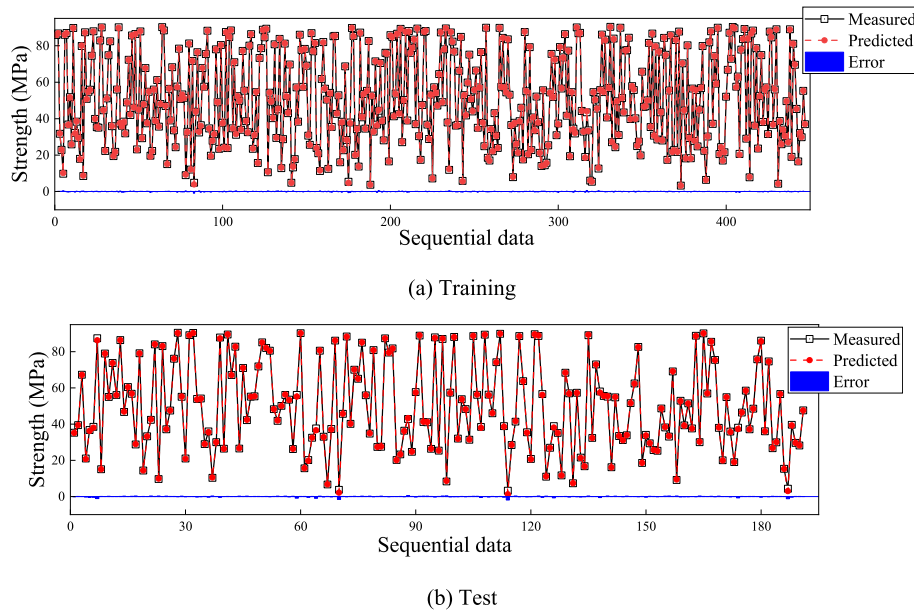


Fig. 6. Sequential data comparison between measured compressive strength and prediction from DCNN.

**Table 4**  
Optimization results of hyperparameter of other learning-based models for strength prediction.

Model	Hyperparameters	Scale	Outcome
ANN	Number of hidden layers	[1, 3]	1
	Activation function	ReLU, Sigmoid, Tanh	Sigmoid
	Regularization strength	[2.24e-8, 223.71]	2.35e-8
	Number of hidden neurons	[1, 300]	10
SVM	Standardize data	Yes, No	Yes
	Box constant	[0.001, 1000]	1.06
	Kernel function	Gaussian, Linear, Quadratic, Cubic	Cubic
GPR	Epsilon	[0.033, 3375.83]	0.382
	Standardize data	Yes, No	Yes
	Sigma	[1e-4, 252.82]	0.003
	Basis function	Constant, Zero, Linear	Constant
	Kernel function	Exponential, Matern 3/2, Matern 5/2, Rational Quadratic	Matern 5/2
EDT	Kernel scale	[0.360, 360]	1.935
	Standardize data	Yes, No	No
	Ensemble method	Bag, LSBoost	Bag
	Number of learners	[10, 500]	13
EDT	Maximum leaf size	[1, 223]	28
	Number of predictors to sample	[1, 6]	5

sulphate attack, we utilize several widely used statistical evaluation metrics to provide a comprehensive evaluation of these learning-based models. These metrics include RMSE, mean absolute error (MAE), and mean absolute percentage error (MAPE). The formula of RMSE has been presented in Eq. (9), while MAE and MAPE are defined by the following formulas.

$$MAE = \frac{1}{n} \sum_{i=1}^n |f_{st}(i) - \hat{f}_{st}(i)| \quad (11)$$

$$MAPE = \frac{1}{n} \sum_{i=1}^n \left| \frac{f_{st}(i) - \hat{f}_{st}(i)}{f_{st}(i)} \right| \quad (12)$$

Among the three indicators, RMSE provides an overall measurement of the accuracy of the predicted strength. MAE measures how closely the predicted strengths align with experimentally measured values, while

MAPE indicates the relative accuracy of predicted strengths. Lower values for these evaluation metrics indicate better predictive accuracy, suggesting that the predicted strengths are closer to the measured strengths of cement-based materials under sulphate attack. Figs. 12–14 illustrate the comparisons of different evaluation indicators of five optimized learning-based models for predicting the compressive strength of cement-based materials subjected to sulphate attack. The comparison is presented in the form of radar plots. It is evident that the proposed method exhibits the best indicators among all the comparative models. For the training data, the values of RMSE, MAE, and MAPE are 0.1504, 0.1049, and 0.0040, respectively. For the test data, the values of RMSE, MAE, and MAPE are 0.3012, 0.1643, and 0.0110, respectively. When comparing the proposed model to ANN, SVM, GPR, and EDT for the training data, the relative errors for RMSE are 675.2%, 439.4%, 389.0%, and 473.9%, respectively. For MAE, the relative errors are 744.1%, 653.5%, 446.6%, and 502.9%, respectively. For MAPE, the relative errors are 669.7%, 493.0%, 405.8%, and 311.3%, respectively. Similarly, for the test data, the relative errors for RMSE are 486.1%, 596.8%, 173.2%, and 234.0%, respectively. For MAE, the relative errors are 759.0%, 634.8%, 288.4%, and 349.6%, respectively. For MAPE, the relative errors are 453.2%, 595.6%, 87.7%, and 66.7%, respectively. These results demonstrate the promising performance of the proposed IPSO optimized DCNN model, which outperforms the other models. The main reason contributing to this phenomenon of results is that in comparison with ANN, SVM, GPR and EDT, the proposed DCNN employs a deeper network architecture. This architecture is adept at extracting high-level features from input data, making it more effective at modeling the highly complex relationship between input variables and the mechanical strength of cement-based materials in adverse environmental conditions. The integration of IPSO for optimizing network hyperparameters further enhances the generalization capability of developed DCNN model. Therefore, it can be considered as a viable solution for the problem of strength evaluation of cement-based materials subjected to sulphate attack in practical applications.

## 6. Robustness and sensitivity analysis

### 6.1. Model robustness analysis

In this section, we investigate the robustness of the proposed hybrid model. We randomly select training data from the entire dataset using

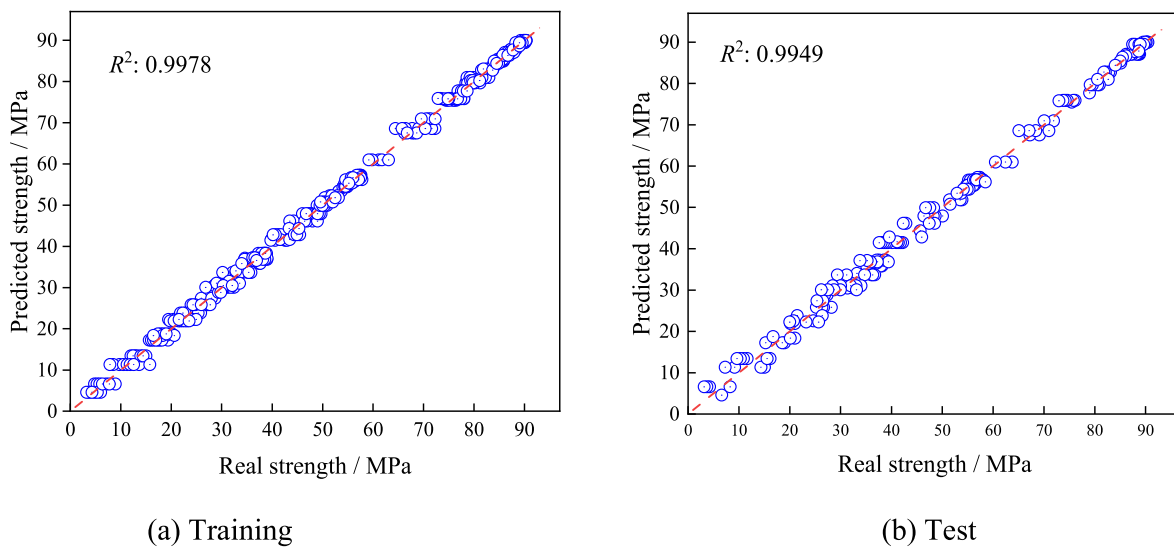


Fig. 7. Regression analysis of ANN model to predict compressive strength of cement-based materials subjected to sulphate attack.

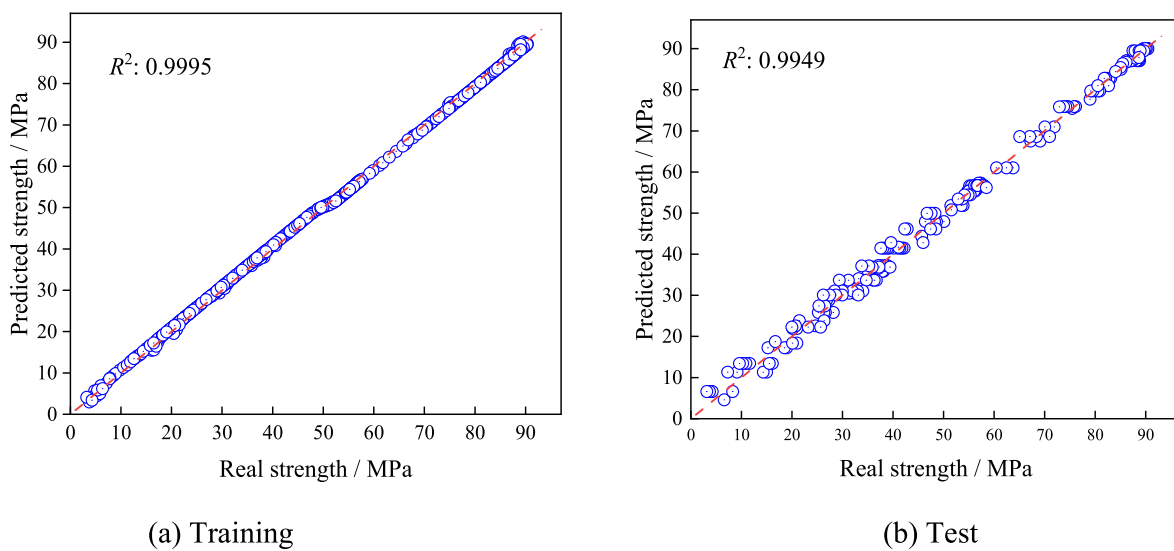


Fig. 8. Regression analysis of SVM model to predict compressive strength of cement-based materials subjected to sulphate attack.

ratios ranging from 0.5 to 0.9 with an increment of 0.1. To assess the robustness of the model, we conduct 20 independent tests for each ratio case. In each test, the training data is used to establish the model, while the test data is employed for evaluating the model performance. The results of the performance of different models in various tests are statistically summarized using box plots, as shown in Fig. 15. The figures labeled (a), (b), (c), and (d) represent the statistical distribution of  $R^2$ , RMSE, MAE, and MAPE, respectively. It is worth noting that as the number of training data increases, the performance of the developed model improves significantly. This improvement is reflected in the evaluation metrics of  $R^2$ , RMSE, and MAE. However, MAPE exhibits an exceptional behavior where the model trained with 80% of the entire dataset outperforms the one trained with 90% of the dataset. Furthermore, as the number of training data increases, the gap between the minimum and maximum errors becomes smaller. When the percentage of training data reaches 80%, the model demonstrates the best robustness. The quartile values of  $R^2$  for this model are 0.99981, 0.99988, and 0.99992 for the 25%, 50%, and 75% quartiles, respectively. The corresponding values for RMSE are 0.2274, 0.2841, and 0.3541, respectively, while for MAE they are 0.0890, 0.0996, and 0.1283, respectively.

Finally, for MAPE, the quartile values are 0.0029, 0.0045, and 0.0055, respectively. Overall, the proposed hybrid model demonstrates a robust capability in predicting the compressive strength of cement-based materials under sulphate attack, despite variations in the training data.

## 6.2. Model sensitivity analysis

In this section, the sensitivity analysis of model inputs is carried out on basis of SHapley Additive exPlanations (SHAP), which is a popular interpretability framework in ML, aiming to explain the predictions made by complex models (Uddin et al., 2023). It provides a unified approach to understanding the importance of features in a model output by assigning a numerical value to each feature, indicating its contribution to the prediction. Based on cooperative game theory, SHAP values quantify the impact of a feature by considering all possible combinations of features and calculating the average change in predictions when a specific feature is included or excluded. This approach ensures fairness and consistency in attributing importance to features. SHAP values offer several advantages for model interpretability. They provide a clear understanding of the factors driving predictions, helping to identify which



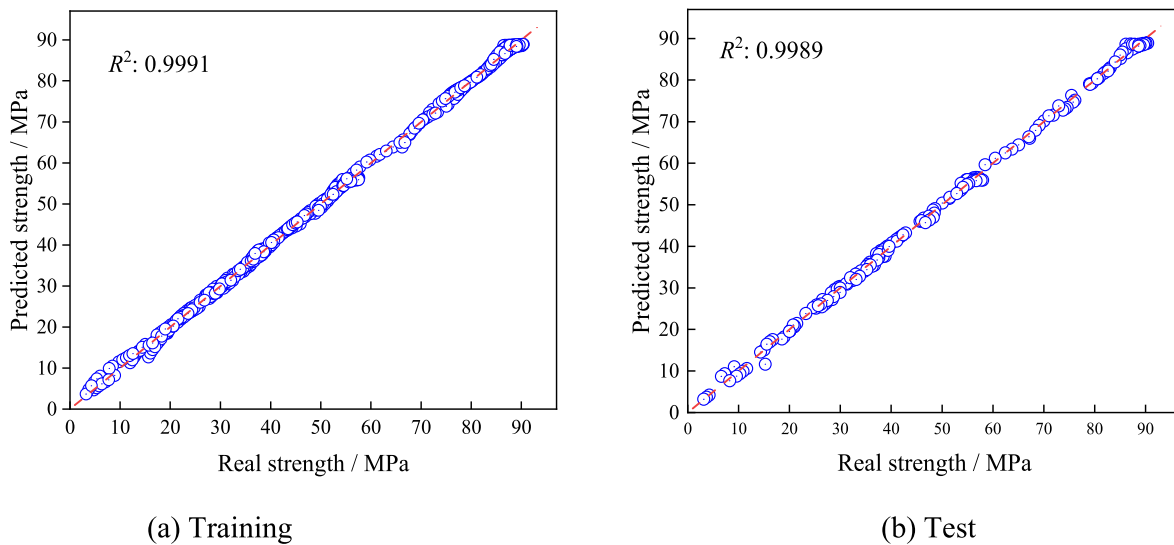


**Fig. 9.** Regression analysis of GPR model to predict compressive strength of cement-based materials subjected to sulphate attack.

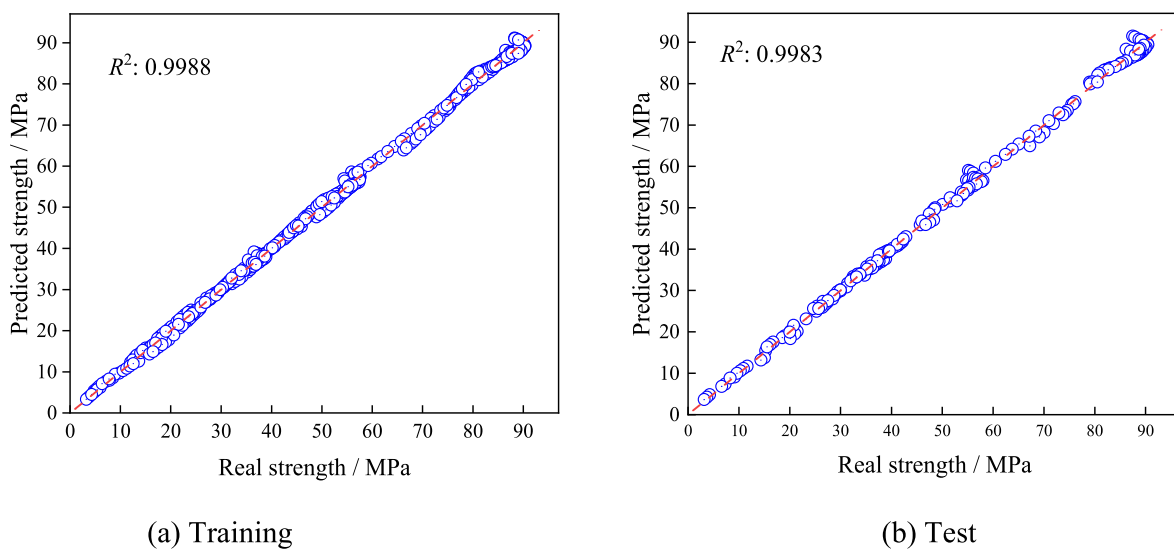


**Fig. 10.** Regression analysis of EDT model to predict compressive strength of cement-based materials subjected to sulphate attack.

features have the most significant influence. Additionally, SHAP values are consistent, meaning that the sum of the individual feature contributions equals the difference between the model output and the expected output. This property allows for reliable comparisons and understanding of feature interactions.

Fig. 16 illustrates the significance of input variables, providing insights into their overall influence on predictions. This significance is determined by averaging absolute SHAP values across entire training data. It is clearly observed that ratio of water to cement (w/c) emerges as the most crucial variable contributing to the compressive strength of cement-based materials subjected to sulphate attack. The primary factor contributing to this phenomenon is the ongoing process of hydration reaction between cement and water in the hardening procedure of cement-based materials (Liu and Sun, 2023). Consequently, ratio of water to cement significantly influences the development of compressive strength. Following is exposure temperature (ET), which exhibits an average absolute SHAP value of around 40% compared to w/c. The sulphate concentration (SSC) ranks next in importance, accounting for approximately one-fifth of the most critical variable. The remaining variables, including superplasticizer (SP), sand and cement, have

relatively minor effects on compressive strength of cement-based materials subjected to sulphate attack. This outcome of sensitivity analysis is similar to the findings in the study conducted by Chen et al. (2018b), which further verifies the reliability of analysis results.

## 7. Conclusions

This research explores the prospect of employing deep learning technology to evaluate the compressive strength of cement-based materials in marine environments. To accomplish this target, a data-driven surrogate model is developed, harnessing the capabilities of DCNN. In order to boost prediction accuracy, the hyperparameters of the DCNN model undergo optimization using the IPSO method during the network training process. The validity and refinement of the proposed method are established through training with experimental data sourced from published literature. The extensive insights derived from this study can be succinctly summarized as follows.

- The proposed DCNN model, with its hyperparameters optimized through the use of IPSO, demonstrates remarkable effectiveness in

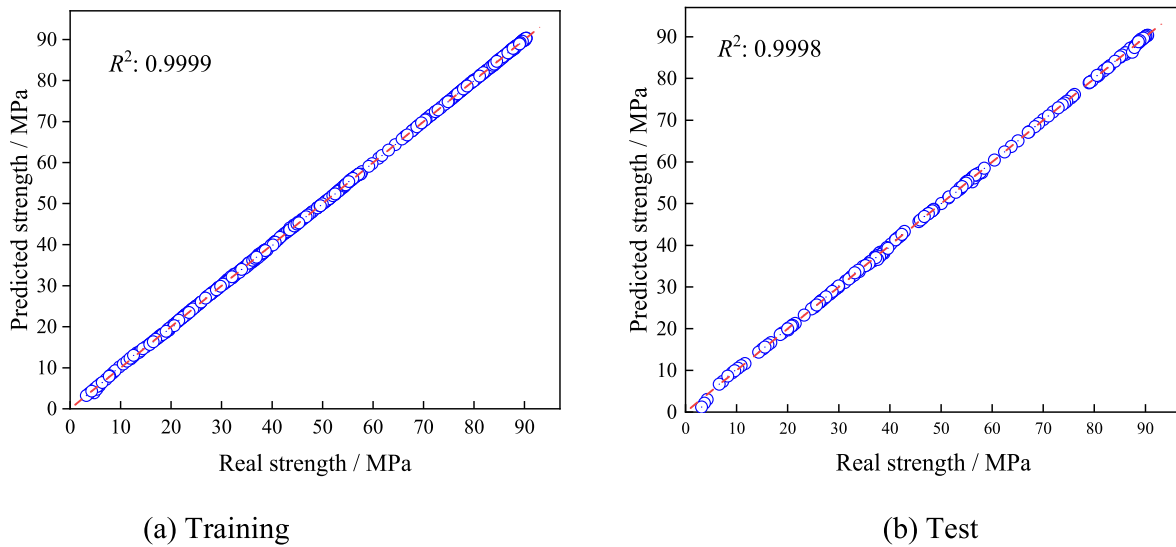


Fig. 11. Regression analysis of Proposed IPSO–CNN model to predict compressive strength of cement-based materials subjected to sulphate attack.

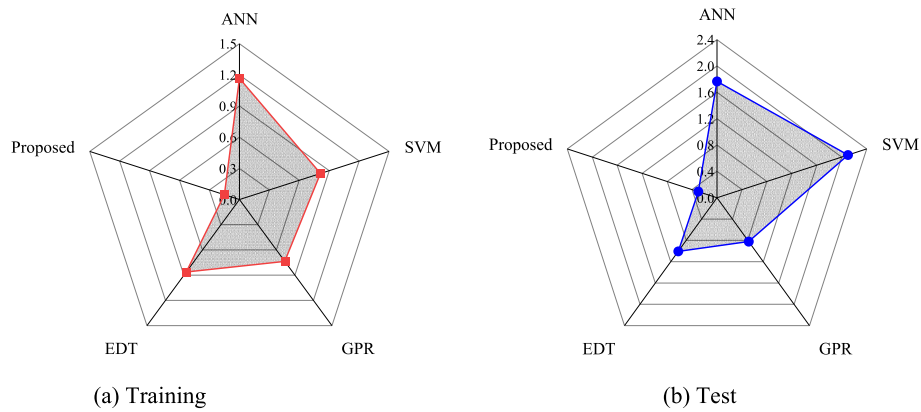


Fig. 12. Comparison of RMSE of different models to predict compressive strength of cement-based materials subjected to sulphate attack.

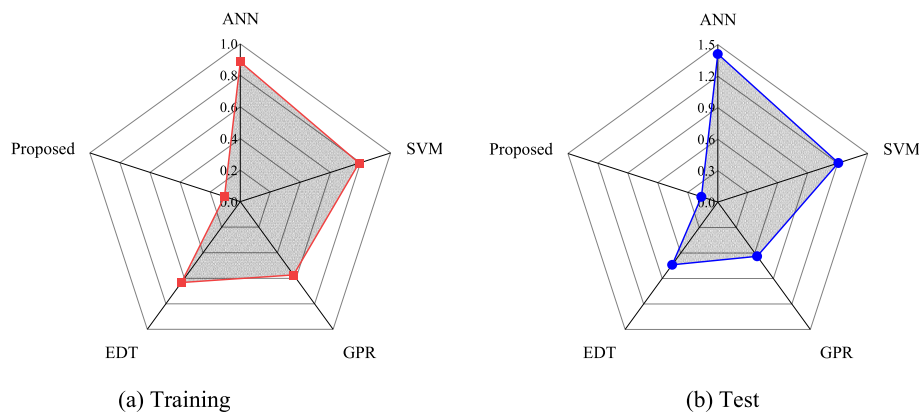


Fig. 13. Comparison of MAE of different models to predict compressive strength of cement-based materials subjected to sulphate attack.

assessing the degradation of cement-based mortars when exposed to sulphate attack.

- In comparison to the optimized ANN, SVM, GPR, and EDT models, the proposed model exhibits superior evaluation indicators, with values of 0.9998, 0.3012, 0.1643, and 0.0110 for  $R^2$ , RMSE, MAE, and MAPE for test data, respectively.
- The results of robustness analysis show that with the increase of number of training data, the performance of the developed model is remarkably enhanced. When the percentage of training data arrives at 80%, the proposed method demonstrates the best performance in predicting mortar strength.
- The analysis of model input sensitivity reveals that the ratio of water to cement, exposure temperature and sulphate concentration are the

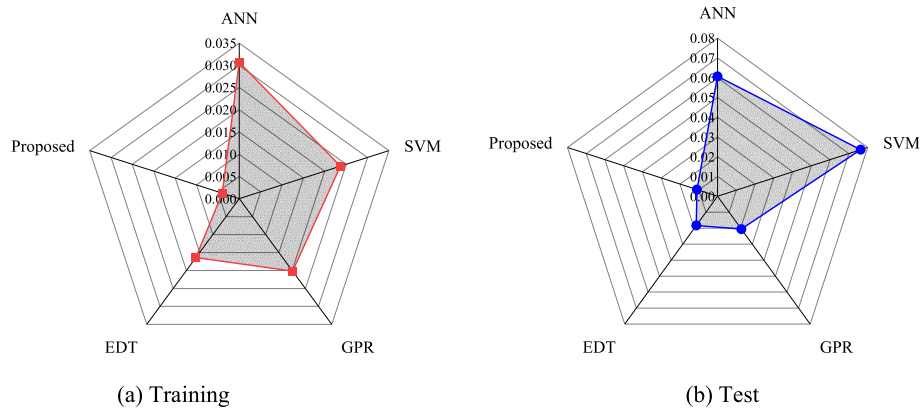


Fig. 14. Comparison of MAPE of different models to predict compressive strength of cement-based materials subjected to sulphate attack.

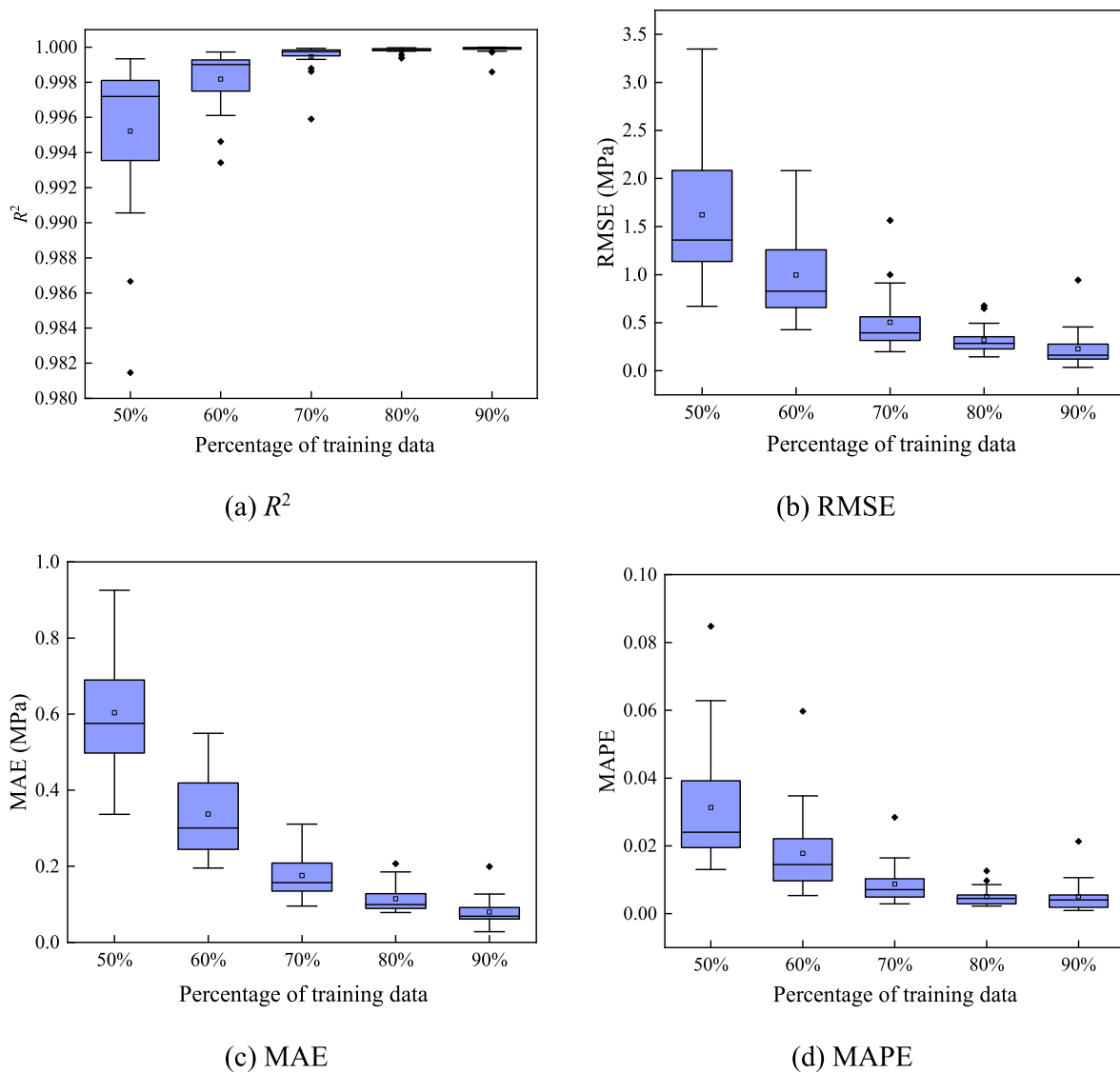


Fig. 15. Statistical distributions of evaluation metrics of different models with different percentages of training data.

primary variables that significantly affect the strength changes of mortar subjected to sulphate attack. Conversely, cement, sand and superplasticizer have relatively minor influences on the development of compressive strength.

Even though the developed model is effective in offering an automated prediction of compressive strength of cement-based materials subjected to sulphate attack, it still exhibits notable drawbacks and limitations that merit thorough consideration in future research. Firstly,

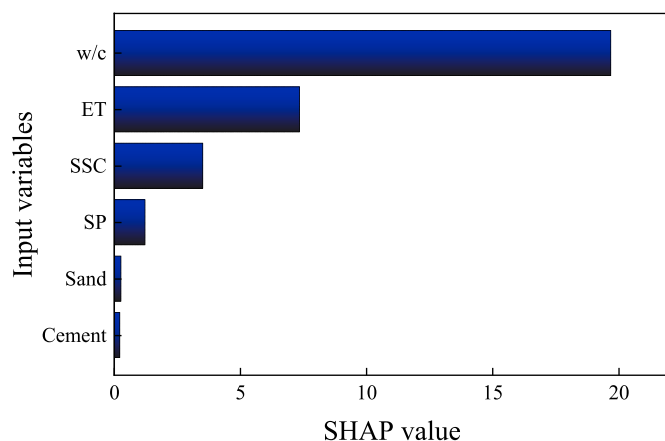


Fig. 16. Sensitivity analysis of model input variables based on SHAP values.

the ranges of input variables in the proposed model should be expanded by adding more experimental data. If a set of new input data is not within the scale of the training dataset, the prediction accuracy of the proposed model cannot be guaranteed. Consequently, more laboratory tests will be conducted in the future to broaden the input variable ranges, and the resulting data will be used for model re-training to enhance its robustness. Additionally, implementing this approach poses challenges and demands considerable time for real application. Consequently, there arises a necessity to create a user-friendly graphical interface aligned with the proposed DCNN model for compressive strength prediction of cement-based materials under sulphate attack. Such an interface would function as a practical tool, empowering researchers to effectively harness the benefits of this methodology.

#### Declaration of competing interest

The authors declare that they have no known competing financial interests or personal relationships that could have appeared to influence the work reported in this paper.

#### Data availability

Data will be made available on request.

#### Acknowledgement

This research was financially supported by the Ministry of Science and Technology of China (Grant No. 2019YFE0112400), the Department of Science and Technology of Shandong Province (Grant No. 2021CXGC011204), the Liaoning provincial key laboratory of Safety and Protection for Infrastructure Engineering, the Central government - Liaoning provincial discovery project. Furthermore, Dr. Huaicheng Chen and Prof. Chunxiang Qian of Southeast University are appreciated for sharing experimental data used in this research.

#### References

Ahmed, H.U., Mohammed, A.S., Mohammed, A.A., 2022. Proposing several model techniques including ANN and M5P-tree to predict the compressive strength of geopolymers incorporated with nano-silica. *Environ. Sci. Pollut. Control Ser.* 29 (47), 71232–71256.

Akbar, A., Kodur, V., Liew, K., 2021. Microstructural changes and mechanical performance of cement composites reinforced with recycled carbon fibers. *Cement Concr. Compos.* 121, 104069.

Akbar, A., Liew, K., 2021. Multicriteria performance evaluation of fiber-reinforced cement composites: an environmental perspective. *Compos. B Eng.* 218, 108937.

Bone, J.R., Stafford, R., Hall, A.E., Herbert, R.J., 2022. The Intrinsic Primary Bioreceptivity of Concrete in the Coastal Environment—A Review. *Developments in the Built Environment*, 100078.

Chen, H., Huang, H., Qian, C., 2018a. Study on the deterioration process of cement-based materials under sulfate attack and drying-wetting cycles. *Struct. Concr.* 19 (4), 1225–1234.

Chen, H., Qian, C., Liang, C., Kang, W., 2018b. An approach for predicting the compressive strength of cement-based materials exposed to sulfate attack. *PLoS One* 13 (1), e0191370.

Congro, M., de Alencar Monteiro, V.M., Brandão, A.L., dos Santos, B.F., Roehl, D., de Andrade Silva, F., 2021. Prediction of the residual flexural strength of fiber reinforced concrete using artificial neural networks. *Construct. Build. Mater.* 303, 124502.

Deng, F., He, Y., Zhou, S., Yu, Y., Cheng, H., Wu, X., 2018. Compressive strength prediction of recycled concrete based on deep learning. *Construct. Build. Mater.* 175, 562–569.

Dharaniya, R., Indumathi, J., Kaliraj, V., 2023. A design of movie script generation based on natural language processing by optimized ensemble deep learning with heuristic algorithm. *Data Knowl. Eng.* 146, 102150.

Gao, M., Kang, Z., Zhang, A., Liu, J., Zhao, F., 2022. MASS autonomous navigation system based on AIS big data with dueling deep Q networks prioritized replay reinforcement learning. *Ocean. Eng.* 249, 110834.

García-Salinas, J.S., Torres-García, A.A., Reyes-García, C.A., Villaseñor-Pineda, L., 2023. Intra-subject class-incremental deep learning approach for EEG-based imagined speech recognition. *Biomed. Signal Process Control* 81, 104433.

Gu, J., Wang, Z., Kuen, J., Ma, L., Shahroudy, A., Shuai, B., Liu, T., Wang, X., Wang, G., Cai, J., 2018. Recent advances in convolutional neural networks. *Pattern Recogn.* 77, 354–377.

Hao, Z., Lu, C., Li, Z., 2023. Highly accurate and automatic semantic segmentation of multiple cracks in engineered cementitious composites (ECC) under dual pre-modification deep-learning strategy. *Cement Concr. Res.* 165, 107066.

Hilloulin, B., Bekrine, I., Schmitt, E., Loukili, A., 2022. Modular deep learning segmentation algorithm for concrete microscopic images. *Construct. Build. Mater.* 349, 128736.

Jaf, D.K.I., Abdulrahman, P.I., Mohammed, A.S., Kurda, R., Qaidi, S.M., Asteris, P.G., 2023. Machine learning techniques and multi-scale models to evaluate the impact of silicon dioxide (SiO<sub>2</sub>) and calcium oxide (CaO) in fly ash on the compressive strength of green concrete. *Construct. Build. Mater.* 400, 132604.

Ji, Y., Chen, A., Chen, Y., Han, X., Li, B., Gao, Y., Liu, C., Xie, J., 2023. A state-of-the-art review of concrete strength detection/monitoring methods: with special emphasis on PZT transducers. *Construct. Build. Mater.* 362, 129742.

Koopialipoor, M., Asteris, P.G., Mohammed, A.S., Alexakis, D.E., Mamou, A., Armaghani, D.J., 2022. Introducing stacking machine learning approaches for the prediction of rock deformation. *Transportation Geotechnics* 34, 100756.

Li, Q.-F., Song, Z.-M., 2022. High-performance concrete strength prediction based on ensemble learning. *Construct. Build. Mater.* 324, 126694.

Liang, C., Qian, C., Chen, H., Kang, W., 2018. Prediction of compressive strength of concrete in wet-dry environment by BP artificial neural networks. *Adv. Mater. Sci. Eng.* 2018.

Ling, H., Qian, C., Kang, W., Liang, C., Chen, H., 2019. Combination of Support Vector Machine and K-Fold cross validation to predict compressive strength of concrete in marine environment. *Construct. Build. Mater.* 206, 355–363.

Liu, G., Sun, B., 2023. Concrete compressive strength prediction using an explainable boosting machine model. *Case Stud. Constr. Mater.* 18, e01845.

Lux, J., Hoong, J.D.L.H., Mahieux, P.-Y., Turcay, P., 2023. Classification and estimation of the mass composition of recycled aggregates by deep neural networks. *Comput. Ind.* 148, 103889.

Ly, H.-B., Nguyen, T.-A., Pham, B.T., 2022. Investigation on factors affecting early strength of high-performance concrete by Gaussian Process Regression. *PLoS One* 17 (1), e0262930.

Lyu, Z., Yu, Y., Samali, B., Rashidi, M., Mohammadi, M., Nguyen, T.N., Nguyen, A., 2022. Back-propagation neural network optimized by K-fold cross-validation for prediction of torsional strength of reinforced concrete beam. *Materials* 15 (4), 1477.

Mohammed, A., Burhan, L., Ghafor, K., Sarwar, W., Mahmood, W., 2021a. Artificial neural network (ANN), M5P-tree, and regression analyses to predict the early age compression strength of concrete modified with DBC-21 and VK-98 polymers. *Neural Comput. Appl.* 33 (13), 7851–7873.

Mohammed, A., Mahmood, W., 2021. Estimating the efficiency of the sandy soils-cement based grout interactions from particle size distribution (PSD). *Geomechanics Geoenviron.* 16 (2), 81–98.

Mohammed, A., Mahmood, W., Ghafor, K., 2020a. Shear stress limit, rheological properties and compressive strength of cement-based grout modified with polymers. *Journal of Building Pathology and Rehabilitation* 5, 1–17.

Mohammed, A., Rafiq, S., Sihag, P., Kurda, R., Mahmood, W., 2021b. Soft computing techniques: systematic multiscale models to predict the compressive strength of HVFA concrete based on mix proportions and curing times. *J. Build. Eng.* 33, 101851.

Mohammed, A., Rafiq, S., Sihag, P., Mahmood, W., Ghafor, K., Sarwar, W., 2020b. ANN, M5P-tree model, and nonlinear regression approaches to predict the compression strength of cement-based mortar modified by quicklime at various water/cement ratios and curing times. *Arabian J. Geosci.* 13, 1–16.

Mohammed, A.K., Hassan, A., Mohammed, A.S., 2023. Predicting the compressive strength of green concrete at various temperature ranges using different soft computing techniques. *Sustainability* 15 (15), 11907.

Moutassem, F., 2022. High Strength Concrete Prestressed Bridges: Exposure Conditions, Mechanical Properties, Modified Design Equations, Parametric Study, and Structural Reliability, Structures. Elsevier, pp. 1369–1382.

- Nazar, S., Yang, J., Amin, M.N., Khan, K., Javed, M.F., Althoey, F., 2023. Formulation of estimation models for the compressive strength of concrete mixed with nanosilica and carbon nanotubes. *Developments in the Built Environment* 13, 100113.
- Nguyen, T.N., Yu, Y., Li, J., Gowripalan, N., Sirivivatnanon, V., 2019. Elastic modulus of ASR-affected concrete: an evaluation using Artificial Neural Network. *Computers and Concrete* 24 (6), 541–553.
- Sarwar, W., Ghafor, K., Mohammed, A., 2019a. Modeling the rheological properties with shear stress limit and compressive strength of ordinary Portland cement modified with polymers. *Journal of Building Pathology and Rehabilitation* 4, 1–12.
- Sarwar, W., Ghafor, K., Mohammed, A., 2019b. Regression analysis and Vipulanandan model to quantify the effect of polymers on the plastic and hardened properties with the tensile bonding strength of the cement mortar. *Results in Materials* 1, 100011.
- Surehali, S., Singh, A., Biligiri, K.P., 2023. A State-Of-The-Art Review on Recycling Rubber in Concrete: Sustainability Aspects, Specialty Mixtures, and Treatment Methods. *Developments in the Built Environment*, 100171.
- Tahwia, A.M., Heniegal, A., Elgamel, M.S., Tayeh, B.A., 2021. The prediction of compressive strength and non-destructive tests of sustainable concrete by using artificial neural networks. *Computers and Concrete, An International Journal* 27 (1), 21–28.
- Ting, M.Z.Y., Ting, T.Z.H., 2023. Deterioration of structural shear connectors in steel-concrete composite exposed to hostile service environments. *J. Build. Eng.*, 106690
- Uddin, M.N., Ye, J., Deng, B., Li, L.-z., Yu, K., 2023. Interpretable machine learning for predicting the strength of 3D printed fiber-reinforced concrete (3DP-FRC). *J. Build. Eng.* 72, 106648.
- Yao, J., Chu, S., 2023. Durability of sustainable marine sediment concrete. *Developments in the Built Environment* 13, 100118.
- Yin, B., Akbar, A., Zhang, Y., Liew, K., 2023. Modeling progressive failure and crack evolution in a randomly distributed fiber system via a coupled phase-field cohesive model. *Compos. Struct.* 313, 116959.
- Yu, L., Chu, H., Zhu, Z., Jiang, L., Dong, H., 2023. Determination of the chloride ion content in concrete under simultaneous chloride and sulphate ion attack. *J. Build. Eng.* 72, 106579.
- Yu, Y., Hoshyar, A.N., Samali, B., Zhang, G., Rashidi, M., Mohammadi, M., 2023a. Corrosion and coating defect assessment of coal handling and preparation plants (CHPP) using an ensemble of deep convolutional neural networks and decision-level data fusion. *Neural Comput. Appl.* 1–22.
- Yu, Y., Li, J., Li, J., Xia, Y., Ding, Z., Samali, B., 2023b. Automated damage diagnosis of concrete jack arch beam using optimized deep stacked autoencoders and multi-sensor fusion. *Developments in the Built Environment* 14, 100128.
- Yu, Y., Liang, S., Samali, B., Nguyen, T.N., Zhai, C., Li, J., Xie, X., 2022. Torsional capacity evaluation of RC beams using an improved bird swarm algorithm optimised 2D convolutional neural network. *Eng. Struct.* 273, 115066.
- Zeng, Z., Wei, Y., Wei, Z., Yao, W., Wang, C., Huang, B., Gong, M., Yang, J., 2022. Deep learning enabled particle analysis for quality assurance of construction materials. *Autom. Construct.* 140, 104374.
- Zhang, C., 2023. The active rotary inertia driver system for flutter vibration control of bridges and various promising applications. *Sci. China Technol. Sci.* 66 (2), 390–405.
- Zhang, C., Kordestani, H., Shadabfar, M., 2023. A combined review of vibration control strategies for high-speed trains and railway infrastructures: challenges and solutions. *J. Low Freq. Noise Vib. Act. Control* 42 (1), 272–291.
- Zhang, C., Mousavi, A.A., Masri, S.F., Gholipour, G., Yan, K., Li, X., 2022. Vibration feature extraction using signal processing techniques for structural health monitoring: a review. *Mech. Syst. Signal Process.* 177, 109175.